



HAL
open science

Swirling spray flames dynamical blow-out induced by transverse acoustic oscillations

Clément Patat, Françoise Baillot, Jean-Bernard Blaisot, Éric Domingues,
Guillaume Vignat, Preethi Rajendram Soundararajan, Antoine Renaud,
Daniel Durox, Sébastien Candel

► **To cite this version:**

Clément Patat, Françoise Baillot, Jean-Bernard Blaisot, Éric Domingues, Guillaume Vignat, et al.. Swirling spray flames dynamical blow-out induced by transverse acoustic oscillations. Symposium on Thermoacoustics in Combustion: Industry meets Academia (soTiC 2021), Sep 2021, Munich, France. hal-03674675

HAL Id: hal-03674675

<https://hal.science/hal-03674675v1>

Submitted on 20 May 2022

HAL is a multi-disciplinary open access archive for the deposit and dissemination of scientific research documents, whether they are published or not. The documents may come from teaching and research institutions in France or abroad, or from public or private research centers.

L'archive ouverte pluridisciplinaire **HAL**, est destinée au dépôt et à la diffusion de documents scientifiques de niveau recherche, publiés ou non, émanant des établissements d'enseignement et de recherche français ou étrangers, des laboratoires publics ou privés.

Swirling spray flames dynamical blow-out induced by transverse acoustic oscillations

Symposium on Thermoacoustics in
Combustion: Industry meets Academia
(SoTIC 2021)
Sept. 6 - Sept. 10, 2021
Munich, Germany
Paper No.: XXX
©The Author(s) 2021

Clément Patat¹, Françoise Baillot¹, Jean-Bernard Blaisot¹, Éric Domingues¹, Guillaume Vignat², Preethi Rajendram Soundararajan², Antoine Renaud², Daniel Durox² and Sébastien Candel²

Abstract

Recent experiments on a laboratory scale annular system comprising multiple injectors (namely, MICCA-Spray) indicate that combustion instabilities coupled with azimuthal modes may induce large amplitude oscillations, which under certain conditions, lead to blow-out of some of the flames established in the system, a phenomenon designated as dynamic blow-out (DBO). An attempt is made in the present investigation to reproduce this phenomenon in a linear array of injectors (namely, TACC-Spray), where the sound field is externally applied to flames established by injector units that are identical to those used in the annular combustor. The sound field is generated by driver units placed on the lateral sides of a rectangular cavity. The pressure level induced in TACC-Spray can reach a peak value of 1700 Pa in a frequency range extending from 680 to 780 Hz, which corresponds to the typical frequency of azimuthal instabilities observed in the annular system. A theoretical model based on dimensional analysis serves to guide the choice of operating conditions that may lead to the DBO phenomenon. Experiments carried out in TACC-Spray and MICCA-Spray are then used to determine the DBO boundary, define the conditions that need to be fulfilled to observe this phenomenon, and gather high-speed visualizations providing some insights on the mechanisms that induce blow-out.

Keywords

Flame blow-out, transverse acoustics, swirling spray flames

Introduction

A considerable amount of research has concerned issues raised by combustion instability. Some of the recent efforts in combustion dynamics has concerned annular configurations that are typically found in aircraft engines and gas turbines. The experimental works [1, 2, 3, 4, 5, 6, 7, 8, 9] have been accompanied by theoretical investigations [10, 11, 12, 13, 14, 15, 16, 17, 18] and by some remarkable large eddy simulations [19, 20]. Since the perimeter is usually the largest dimension in these combustor geometries, azimuthal modes feature the lowest eigenfrequencies, which fall in the range where combustion is most sensitive to disturbances. As a consequence, these systems are susceptible to instabilities coupled by azimuthal modes. If this happens in a real system, this may lead to serious consequences, including mechanical vibration, cyclic fatigue, enhanced heat fluxes to the combustor walls, and in extreme cases, mechanical degradation and possibly failure. There are also instances where the oscillation reaches an amplitude that can lead to flashback. Many of these issues are considered in research reported in recent reviews (see [21, 22, 23, 24] on azimuthal instabilities).

A series of more recent experiments have been carried out in annular systems allowing investigations of instabilities coupled by azimuthal modes. Much of these data originates from two laboratory scale annular systems with optical access to the combustion region, one earlier located in Cambridge and later in NTNU [3, 4], while the other (MICCA-Spray) is operated at EM2C lab [6, 8, 9, 25, 26].

These two facilities reproduce in an idealized fashion, the conditions that prevail in gas turbines and jet engines. The two systems comprise multiple injectors arranged in an annular chamber. While the first is essentially fed with premixed reactants (air and ethylene), MICCA-Spray may be operated with premixed air and propane or may be fed with liquid fuel (n-heptane or dodecane) that is injected in the form of sprays. Flame stabilization in the Cambridge-NTNU system is assured by central bluff bodies with a relatively low swirl number. In the MICCA-Spray device, most investigations have been carried out with swirling injectors fed by premixed reactants and more recently by liquid fuels atomized as a spray of droplets.

These experimental facilities have provided considerable insight on the processes driving and coupling azimuthal instabilities. Recent combustion instability experiments carried out in MICCA-Spray have revealed an intriguing

¹CORIA, CNRS, Université de Rouen, 76801 Saint-Étienne-du-Rouvray, France

²EM2C lab, CNRS and CentraleSupélec, University Paris-Saclay, 91192 Gif-sur-Yvette, France

Corresponding author:

Sébastien Candel, EM2C lab, CNRS and CentraleSupélec, University Paris-Saclay, 91192 Gif-sur-Yvette, France;

Françoise Baillot, CORIA, CNRS, Université de Rouen, 76801 Saint-Étienne-du-Rouvray, France

Email: sebastien.candel@centralesupelec.fr; francoise.baillot@coria.fr
Present address of G. Vignat: Stanford University, Department of Mechanical Engineering, Stanford, CA 94305, USA.

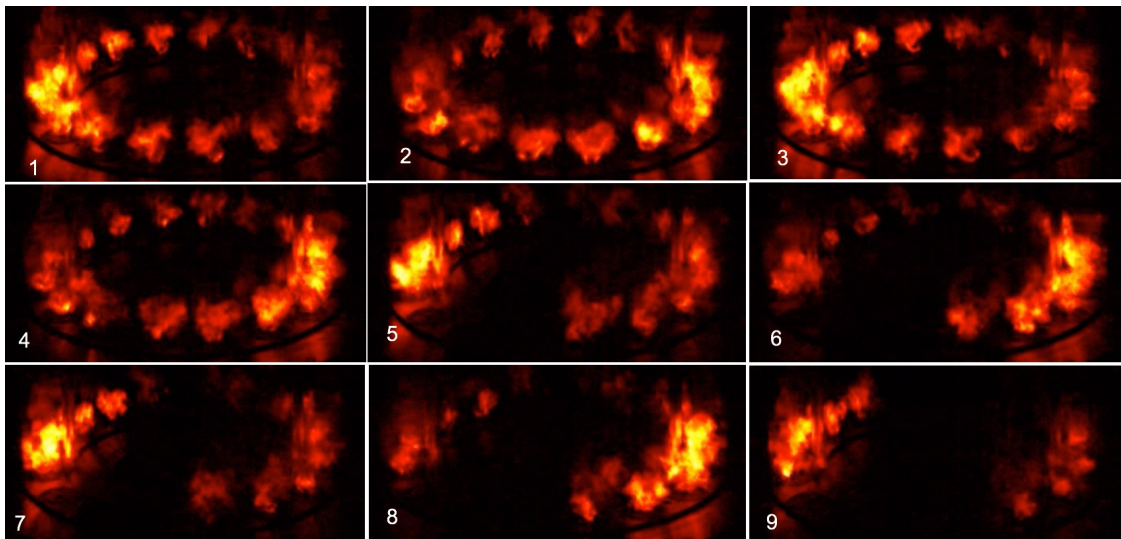


Figure 1. Dynamical blow-out in MICCA-Spray. Images show the progressive blow-out of the flames located near the pressure nodal line as the acoustic pressure amplitude grows up to 4000 Pa [27].

phenomenon when the oscillation amplitude was taking large values, typically in excess of 2% to 3% of the chamber pressure [9]. Under these conditions, some of the flames established in the annular combustor were extinguished, as illustrated in Fig. 1 for an acoustic pressure amplitude of 4000 Pa. Further analysis indicated that this partial blow-out occurred in the vicinity of the pressure nodal line, where the transverse velocities associated with the azimuthal mode reach their maximum level inducing an intense sweeping motion. Under these conditions, the combustion process is disrupted, inducing the complete extinction of flames located in the neighborhood of the nodal line. The time duration of this phenomenon was found to encompass about 100 ms, corresponding to about 70 cycles of oscillation. After this blow-out, the amplitude of oscillation in the chamber diminishes and the flames are established again. The process may then be repeated, leading to a new partial blow-out. This phenomenon, designated in what follows as dynamical blow-out (DBO) was the subject of a further investigation [27], and it was found that the flame extinction was accompanied by a notable distortion of the pressure field and simultaneously by an increase of the shift in the resonance frequency. It was also possible to estimate the velocity fluctuation amplitude corresponding to the initial flame extinction.

The objective of the present study is to pursue the analysis of the DBO by making use of a configuration designated as TACC-Spray, in which the acoustic modulations are imposed to the flame by external means. In essence, this consists in placing a linear array of swirl spray injectors in a rectangular system. A transverse acoustic mode is generated by driver units located on the lateral boundaries of this facility. The central flame of the injector array can then be placed at the pressure nodal line, corresponding to the maximum transverse acoustic velocity. It is then possible to augment the level of oscillation and examine the process leading to flame blow-out. One advantage of this procedure is that the acoustic level is fully controlled, thus facilitating the detailed investigation of the DBO. It is in particular possible to decouple the level of the acoustic mode and the combustion operational conditions, a feature that is not accessible in the

annular combustor MICCA-Spray where the acoustic level is governed by the coupling between acoustics and combustion.

The idea of using linear arrays of injectors to represent a sector of an annular system is not new. This has already been exploited by O'Connor and Lieuwen [28, 29], by Wong and Steinberg [30] or by Lespinasse et al. [31, 32]. In these last references, a premixed “V” flame is placed in a transverse acoustic field. When placed at the pressure antinodal line, the flame is led to execute an axial motion. There are also nonlinear features with lateral ejections of fluid at the injector outlet [32]. In the vicinity of the pressure nodal line, the flame is periodically swept in the transverse direction. If the injection unit comprises a swirler, helical perturbations result from the interaction of the transverse acoustic velocities with the shear regions and with the vortex breakdown process [28, 29]. Transverse waves acting on the upstream side of the injector unit may also induce a rotational motion of the flames at the injector outlets, associated to asymmetric velocity field perturbations in the injector nozzles [33]. The capacity of flames to maintain the combustion process under intense transverse velocities induced by an acoustic mode was investigated by Lespinasse et al. [31], where it is shown that premixed “V” flames placed at a pressure nodal line are more sensitive to blow-off than the same flames placed at a pressure antinodal line. These flames were stabilized on a cylindrical rod having a diameter $d = 3$ mm placed in a premixed flow at a bulk velocity $U_b = 2$ ms⁻¹. Flame extinction was obtained, for example, at a pressure amplitude of 100 Pa at two resonance frequencies $f_0 = 506$ Hz and $f_0 = 1012$ Hz. The transverse velocity at the pressure node could be estimated to be about 0.2 ms⁻¹, corresponding to 10% of the bulk velocity. The response of a linear array of swirling spray flames centered on a pressure antinode of a 2T1L resonant mode was examined in the new facility TACC-Spray [34], where the flames are stabilized without any bluff-body and without the help of side walls.

Further references dealing with combustion instabilities and coupling with transverse acoustic modes are reviewed in [23]. It appears that there are no detailed investigations of the DBO process for swirling spray flames subjected to a

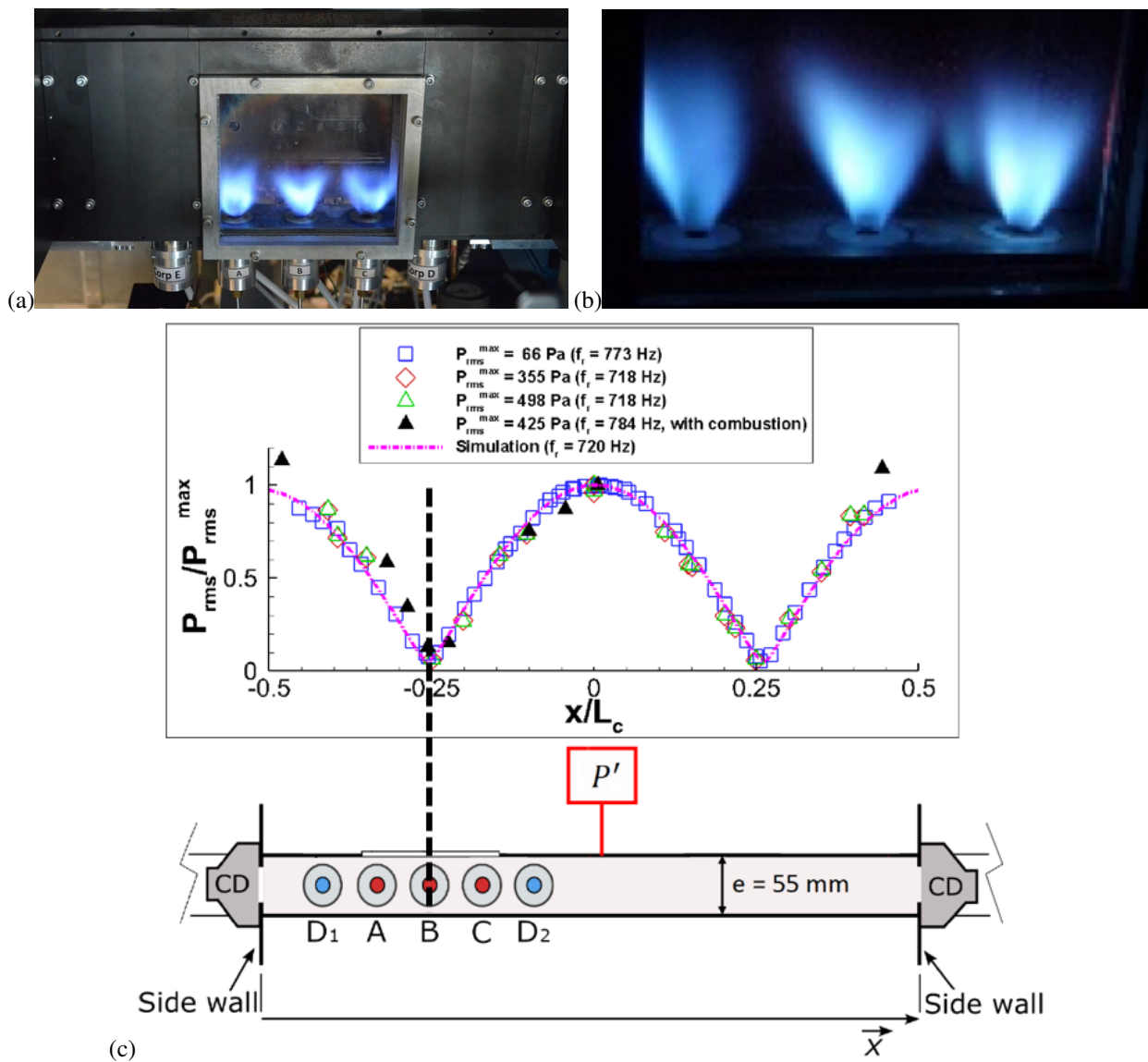


Figure 2. (a) The TACC-Spray setup showing the injector array and lateral quartz window, (b) close-up view of the three flames, (c) transverse acoustic field inside the cavity and top view of the TACC-Spray setup. The central flame (injector B) is placed at a velocity antinode. The pressure fluctuation P' is measured at the central pressure antinode.

transverse acoustic field. The objective of the present work is to bring new insight into this process by combining well controlled experiments with a theoretical framework initially proposed in [35] but modified in the present article.

This article begins with a brief description of the experimental configuration. The blow-out process is examined in the framework of a theoretical model, which serves to guide the experimental investigation. Experiments indicate that flame blow-out is observed when the pressure amplitude reaches high levels and when the flame is located near the transverse velocity antinodal line. This point is examined in more detail for two mass flow rates of air.

Experimental set-up and diagnostics

The TACC-Spray set-up, shown in Fig. 2, comprises a rectangular chamber. The top of the chamber is surmounted by a convergent part which prevents the entrainment of surrounding air. Its exhaust is open to the atmosphere. An array of five injection units is mounted in the chamber

backplane with a spacing that is equal to that used in the MICCA-Spray experiment. They are equipped with tangential swirlers of type 716, identical to those of MICCA-Spray (see [27] for further details about the swirler). The three central ones inject air and n-heptane while the two lateral ones supply only air, as they act as stabilizers of the lateral flames. This original arrangement allows to stabilize the lateral flames far from the side walls, which puts the central flame in an environment similar to that of MICCA-Spray at any location of the acoustic field. Two compression drivers Beyma CP850ND (marked as CD in Fig. 2) are fixed on the side walls, facing each other such that their common acoustic axis which passes through their centers is at 90 mm from the chamber backplane. They are characterized by a wide frequency range (0.5–20 kHz). The excitation signals are delivered by a Hameg HM8150 signal generator, an IMG Stageline frequency filter and a Peavey PV900 amplifier. Here, the acoustic pressure P' is measured with a B&K type

4182 microphone placed at the central pressure antinode of the chamber.

The vertical side walls holding the driver units are placed on rails and the front walls are made of plates of height $h_c = 200$ mm and different lengths, which allows to vary the chamber length l_c and ensure acoustic resonance at a selected frequency f for a frequency in the range 680-780 Hz, corresponding to the DBO frequency range in MICCA-Spray. A transverse mode is generated in the rectangular chamber, with peak amplitude levels that may reach 1700 Pa. This is used to locate the pressure, velocity or intensity antinode so that it coincides with the central injector. High-speed imaging of the OH* radical is performed at an acquisition rate of 10000 fps with a Phantom V2012 camera equipped with a Lambert HiCATT 25 intensifier, a UV-105 mm lens and a UG11 filter.

Theoretical framework

The general ideas that were followed in [35] to derive a theoretical model for the DBO phenomenon are now used to guide the blow-out experiments in TACC-Spray. Blow-out takes place when the central injector is located at a pressure node of the resonant acoustic field, where the transverse velocity v'_x reaches maximum values. The data from MICCA-Spray indicate that DBO requires high amplitude oscillations. It is also found that the transverse velocity induced by the acoustic field displaces the flames in the transverse direction. This modifies the heat release rate in the flames located near the pressure nodal line where the transverse velocity reaches its maximum. In the initial model, the parameters influencing the blow-out were as follows : $d, U_b, \tau_c, v'_x, \omega = 2\pi f$, and the swirl number S . The conversion time $\tau_c = \tau_m + \tau_v + \tau_{ch}$ includes a mixing time τ_m , a vaporization time τ_v and a chemical time τ_{ch} . Mixing is essentially governed by turbulence, vaporization depends on the droplet diameters and clustering in the spray, while the chemical conversion is a function of the local equivalence ratio ϕ . Dimensional analysis indicates that there are four dimensionless groups that may be written as v'_x/U_b , the relative velocity perturbation, $v'_x/(\omega d)$, the ratio of the transverse displacement to the injector outlet diameter, $(\tau_c U_b)/d$, the ratio of the chemical conversion time to a mechanical time d/U_b and S , the swirl number measuring the rate of rotation with respect to the axial flow velocity. The flame extinction is then formally governed by a criterion that may be cast in the form:

$$\psi_1 \left(\frac{v'_x}{U_b}, \frac{v'_x}{\omega d}, \frac{\tau_c U_b}{d}, S \right) > 0 \quad (1)$$

It was initially considered that the relative transverse displacement amplitude $v'_x/(\omega d)$ was governing the flame extinction process. When this ratio is sufficiently large, the central recirculation zone which anchors the flame is significantly perturbed, destabilizing the flame and inducing blow-out. However, $v'_x/(\omega d)$ is dependent on v'_x/U_b and the inverse of the Strouhal number St defined by $St = \omega d/U_b$. So, it may be interesting to replace the second dimensionless group by the Strouhal number. The influence of frequency on the process is then reflected by this important dimensionless

number. The extinction condition may then be rewritten in the form:

$$\frac{v'_x}{U_b} > \psi_2 \left(St, \frac{\tau_c U_b}{d}, S \right) \quad (2)$$

It is known that the parameter $(\tau_c U_b)/d$ that will be designated from here on by b , typically determines the stability of a combustion system. When this parameter is smaller than a critical value corresponding to static blow-out, say b_* of the order of one, the conversion time is shorter than the mechanical time and the flame is stabilized. When b exceeds b_* , the flame is extinguished. This is equivalent to say that the Damköhler number should exceed a critical value for flame stabilization (*i.e.* $Da > Da_c$). The difference $b_* - b$ then measures the stability margin and may be used in place of the dimensionless group b . One may then separate the right hand side in expression (2) in two parts, the first reflecting the state of rotation and flow response $\psi_3(S, St)$ while the second represents the stability margin in the form $(b_* - b)^n$. The dynamical blow-out criterion then takes the form:

$$\frac{v'_x}{U_b} > \psi_3(S, St)(b_* - b)^n \quad (3)$$

This criterion slightly differs from that proposed in [35] in that it puts the accent on the transverse velocity disturbance and on the stability margin of the flame. The function ψ_3 portrays the swirling flow characterized by the swirl number S and its response to external modulations through a Strouhal number. For a fixed injector and a broadband receptivity to incident disturbances, one may consider that ψ_3 is a constant so that the criterion is essentially controlled by the stability margin $(b_* - b)^n$ where n may be obtained from experiments. If the flame is close to blow-off, it may be easily perturbed by the external acoustic field. If the stability margin is greater, then the combustion process will be less easily perturbed. In the previous expression, $b = U_b \tau_c/d$ defines the stability of the flame and one may note that v'_x/U_b has to be sufficiently large if the acoustic field is to play a role and induce flame blow-off. This analysis may be tested by changing the value of b to vary the stability margin of the flame. For a fixed injector geometry, this may be achieved by changing the bulk velocity U_b or by changing the conversion time τ_c . When τ_c is increased, the stability margin is reduced. It is most convenient to augment the chemical time by operating under leaner conditions *i.e.* by reducing the equivalence ratio and operating near the lean blow-out limit. This is illustrated in Fig. 3.

Diagrams in Fig. 3 may be used to guide the exploration of the DBO phenomenon. The central idea is to explore flames that have a narrow margin with respect to the lean blow-out limit. The acoustic level is fixed and the equivalence ratio is progressively decreased until flame blow-out. This scheme is repeated for higher acoustic levels until the maximum achievable level is reached. The corresponding equivalence ratio ϕ_{lim} is that which requires the highest achievable level of pressure oscillation, *i.e.* the highest level of transverse velocity fluctuation. Beyond that point, the system cannot provide a level of oscillation that will lead to blow-out.

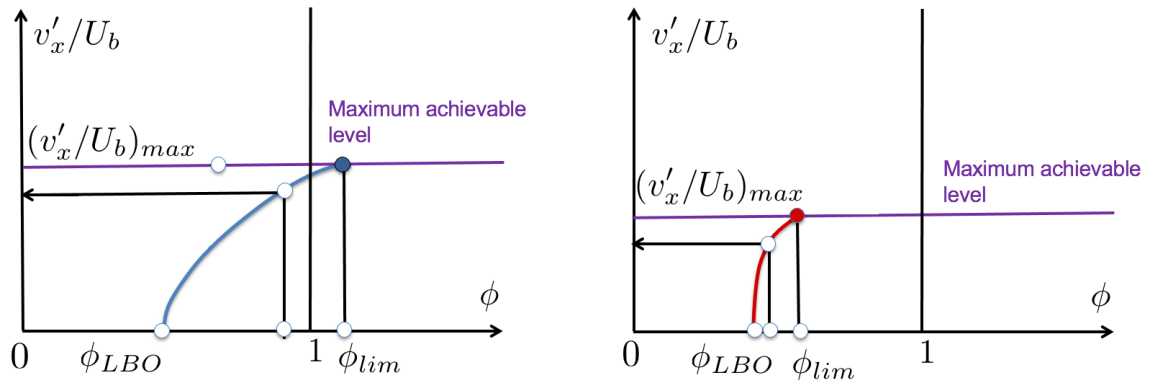


Figure 3. Dynamical flame blow-out conditions may be determined by changing the equivalence ratio to vary the stability margin. When this ratio reaches the lean blow-out limit, the flame is extinguished. The range of equivalence ratios between ϕ_{LBO} and a limit value ϕ_{lim} may be explored and the level of transverse oscillation that leads to extinction may be determined. Beyond ϕ_{lim} , the level of transverse velocity fluctuation exceeds the maximum achievable value and this range cannot be explored. These diagrams only consider lean operating conditions. Left: Low bulk velocity case. The flame is not very well anchored and extinction may be observed over an extended range of equivalence ratios limited by the maximum achievable level of transverse velocity fluctuation. Right: High bulk velocity case. Flame anchoring is improved and the maximum achievable level of relative transverse velocity oscillation is reduced. The range of equivalence ratios in which DBO may be observed is diminished.

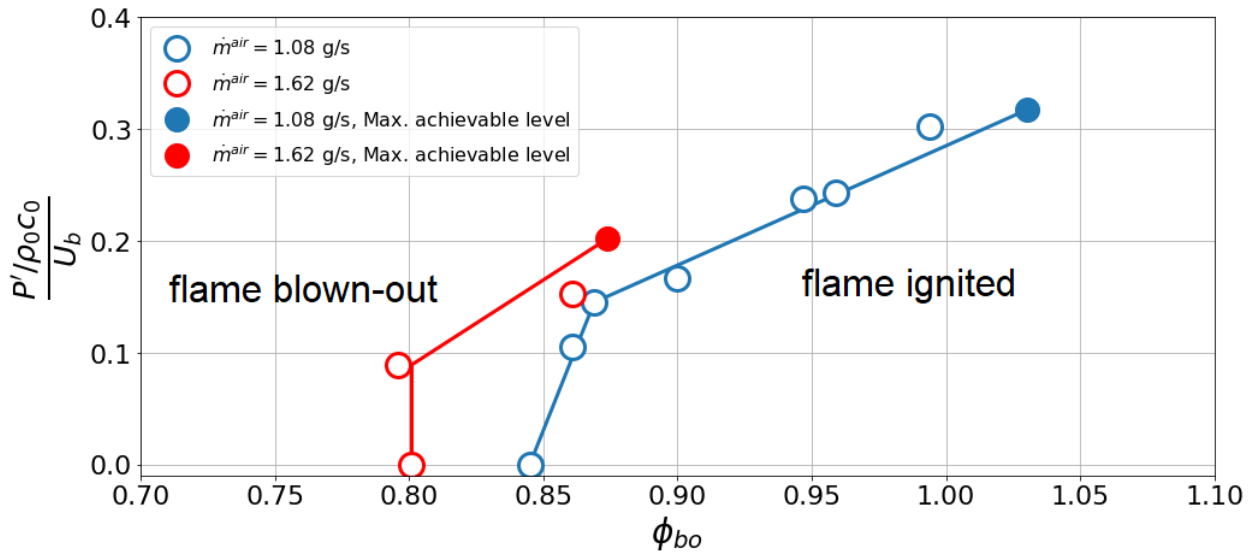


Figure 4. Flame blow-out boundary for two different regimes of operation. Swirler type: 716, n-heptane fuel. The blue symbols correspond to $U_b = 17.8$ m/s, $f = 760$ Hz and the red symbols correspond to $U_b = 26.7$ m/s, $f = 755$ Hz. Filled symbols indicate the maximum achievable level of $P' / (\rho_0 c_0 U_b)$.

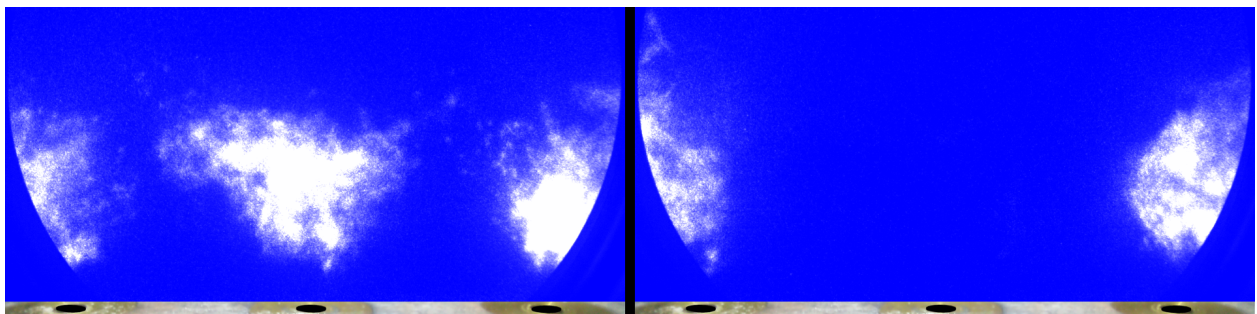


Figure 5. Images of the flames in TACC-Spray. Left: 0.25 s before blow-out; right: 0.03 s after blow-out of the central flame. $U_b = 17.8$ m/s, $\phi = 0.96$, $f = 760$ Hz, $P' / (\rho_0 c_0 U_b) = 0.24$.

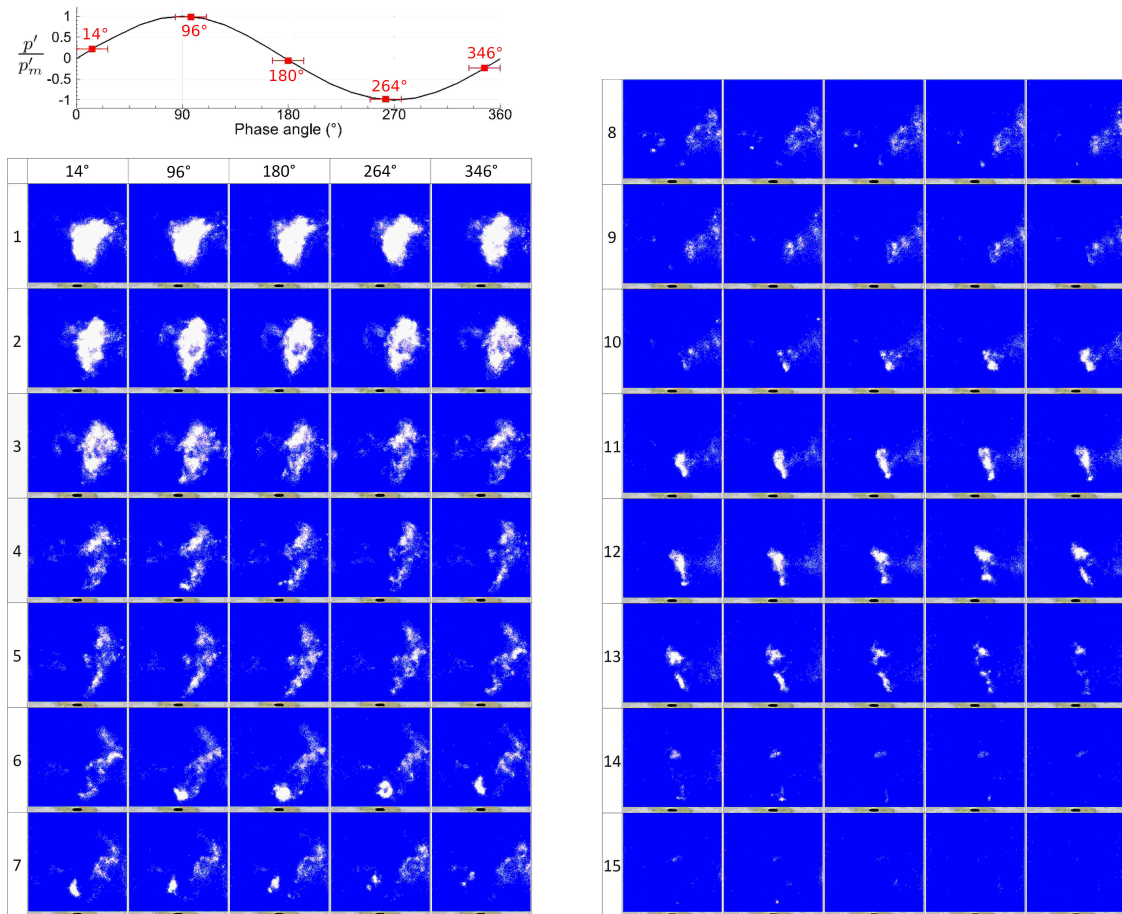


Figure 6. Images of the flame blow-out process extracted from a high speed film recorded at 10000 fps for $U_b = 17.8$ m/s, $\phi = 0.96$, $f = 760$ Hz. The process is decomposed in 15 acoustic cycles (rows), and five images per cycle for the same phase angles (columns).

Flame blow-out induced by high amplitude oscillations

It is now interesting to examine results of blow-out experiments carried out for two different mass flow rates of air. The corresponding blow-out boundaries are plotted in Fig. 4.

When the bulk velocity is low ($U_b = 17.8$ m/s) corresponding to the blue line, the maximum level of fluctuation may reach a value of 32 %. The flame is also not very well anchored because atomization probably produces bigger droplets and the vaporization time is high, reducing the Damköhler number. In this case, transverse acoustic oscillations induce blow-out at equivalence ratios as high as 1.03. This situation corresponds to that shown schematically in Fig. 3 (left). When the bulk velocity is increased ($U_b = 26.7$ m/s) atomization is improved, vaporization time is reduced and flame anchoring is enhanced. The achievable level of velocity fluctuation is reduced to about 20%. In this case, DBO is only observable in a more limited range of equivalence ratios, as shown schematically in Fig. 3 (right). Moreover, blow-out occurs at the same equivalence ratio without acoustics and for a relative velocity perturbation of 9%, which is not observed for the low bulk velocity.

The DBO process may now be examined by making use of high speed imaging of OH*. As shown in Fig. 5, the two lateral flames are still present a short time after blow-out

of the central flame, which is thus the only one concerned by DBO. Since it is located at the velocity antinode, it experiences a transverse velocity modulation of stronger amplitude compared to the lateral flames. This indicates that DBO at the pressure nodal line observed in MICCA-Spray can be reproduced in TACC-Spray. A time analysis of the DBO process of the central flame in TACC-Spray is provided in Fig. 6, which shows a map of images extracted from a film recorded at 10000 frames per second. The blow-out requires about 21 ms corresponding to about 15 acoustic cycles at 760 Hz. During the DBO process, the flame is extinguished by its upper part, the OH*-intensity of which decreases from cycle no. 1 to cycle no. 5. At the same time, the flame is laterally displaced away from the axis of the injector (e.g., images of cycle no. 5) while its stabilization height from the burner is practically unmodified. This process is accompanied by the occasional reactivation of the stabilization point (e.g., in the beginning of cycle no. 6 and the end of cycle no. 10), but these puffs of OH*-intensity are not capable to reignite the entire flame, which leads to a complete blow-out in cycle no. 15. It is interesting to note that the duration of the process is of the order of ten times the residence time in the inner recirculation zone that anchors the flame. This region is progressively modified by the transverse velocity field and the flame foot displaced in the lateral direction is subjected to

cooler gases and a reduced level of fuel that are less favorable to stabilization.

Conclusion

Experiments have been carried out in a system comprising an array of swirling injectors fed with liquid n-heptane and air placed in a rectangular configuration operating at atmospheric pressure. This configuration may be modulated by transverse acoustic modes generated by a set of driver units located on the lateral sides of the system. The pressure oscillation may reach peak values of the order of 1700 Pa peak (about 2% of the chamber pressure). Experiments reveal that these high acoustic levels induce a strong transverse motion in the neighborhood of the pressure nodal line. Experiments indicate that the combustion process markedly changes when the position of the central injector coincides with a pressure antinode or when it corresponds to a nodal line. In this latter case, when the pressure oscillation amplitude exceeds a certain threshold, the flame senses maximum transverse velocity fluctuations that produce a dynamical extinction. A mechanism is proposed for the flame extinction process that defines a critical value for the transverse velocity amplitude with respect to the injection velocity. The data reported in this article provide new insights on the dynamical blow-out that results from excessive levels of acoustic oscillation. The data can serve to guide modeling and simulation of interactions between acoustics and combustion.

Acknowledgements

This work was partially supported by project FASMIC (ANR16-CE22-0013) of the French National Research Agency (ANR), and by the European Union's Horizon 2020 research and innovation programme, "Annulight" with grant agreement no. 765998. The authors wish to thank RENADIAG for the technical support provided to this research.

References

- [1] Fanaca D, Alemela PR, Hirsch C et al. Comparison of the Flow Field of a Swirl Stabilized Premixed Burner in a Annular and a Single Burner Combustion Chamber. *Journal of Engineering for Gas Turbines and Power* 2010; 132(7): 071502.
- [2] Moeck JP, Paul M and Paschereit CO. Thermoacoustic Instabilities in an Annular Rijke Tube. In *ASME Conference Proceedings, Paper GT 2010-23577*. Glasgow, UK.
- [3] Worth NA and Dawson JR. Self-excited circumferential instabilities in a model annular gas turbine combustor: Global flame dynamics. *Proceedings of the Combustion Institute* 2013; 34(2): 3127–3134.
- [4] Worth NA and Dawson JR. Modal dynamics of self-excited azimuthal instabilities in an annular combustion chamber. *Combustion and Flame* 2013; 160(11): 2476–2489.
- [5] Bourgooin JF, Durox D, Schuller T et al. Ignition dynamics of an annular combustor equipped with multiple swirling injectors. *Combustion and Flame* 2013; 160(8): 1398–1413.
- [6] Bourgooin JF, Durox D, Moeck J et al. Self-sustained instabilities in an annular combustor coupled by azimuthal acoustic modes. In *Proceedings of ASME Turbo Expo, Paper GT2013-95010*. San Antonio, Texas, USA.
- [7] Worth NA, Dawson JR, Sidey JAM et al. Azimuthally forced flames in an annular combustor. *Proceedings of the Combustion Institute* 2016; 36(3): 3783–3790.
- [8] Prieur K, Durox D, Schuller T et al. A hysteresis phenomenon leading to spinning or standing azimuthal instabilities in an annular combustor. *Combustion and Flame* 2017; 175(): 283–291.
- [9] Prieur K, Durox D, Schuller T et al. Strong Azimuthal Combustion Instabilities in a Spray Annular Chamber With Intermittent Partial Blow-Off. *Journal of Engineering for Gas Turbines and Power* 2018; 140(3): 031503.
- [10] Evesque S, Polifke W and Pankiewicz C. Spinning and azimuthally standing acoustic modes in annular combustors. In *AIAA Conference Proceedings Paper 2003-3182*.
- [11] Ghirardo G and Juniper M. Azimuthal instabilities in annular combustors: standing and spinning modes. *Proceedings of the Royal Society A: Mathematical, Physical and Engineering Science* 2013; 469: 2013032.
- [12] Noiray N and Schuermans B. On the dynamic nature of azimuthal thermoacoustic modes in annular gas turbine combustion chambers. *Proceedings of the Royal Society A: Mathematical, Physical and Engineering Science* 2013; 469: 20120535.
- [13] Bauerheim M, Parmentier JF, Salas P et al. An analytical model for azimuthal thermoacoustic modes in an annular chamber fed by an annular plenum. *Combustion and Flame* 2014; 161: 1374–1389.
- [14] Bauerheim M, Salas P, Nicoud F et al. Symmetry breaking of azimuthal thermo-acoustic modes in annular cavities: a theoretical study. *Journal of Fluid Mechanics* 2014; 760: 431–465.
- [15] Ghirardo G, Juniper M and Moeck JP. Weakly nonlinear analysis of thermoacoustic instabilities in annular combustors. *Journal of Fluid Mechanics* 2015; 805: 52–87.
- [16] Bothien M, Noiray N and Schuermans B. Analysis of azimuthal thermo-acoustic modes in annular gas turbine combustion chambers. *Journal of Engineering for Gas Turbines and Power* 2015; 137: 061505.
- [17] Laera D, Schuller T, Prieur K et al. Flame Describing Function analysis of spinning and standing modes in an annular combustor and comparison with experiments. *Combustion and Flame* 2017; 184: 136–152.

- [18] Moeck JP, Durox D, Schuller T et al. Nonlinear thermoacoustic mode synchronization in annular combustors. *Proceedings of the Combustion Institute* 2019; 37(4): 5343–5350.
- [19] Wolf P, Balakrishnan R, Staffelbach G et al. Using LES to Study Reacting Flows and Instabilities in Annular Combustion Chambers. *Flow, Turbulence and Combustion* 2012; 88(1-2): 191–206.
- [20] Wolf P, Staffelbach G, Gicquel L et al. Acoustic and large eddy simulation studies of azimuthal modes in annular combustion chambers. *Combustion and Flame* 2012; 159: 3398–3413.
- [21] Candel S. Combustion dynamics and control : progress and challenges. *Proceedings of the Combustion Institute* 2002; 29(1): 1–28.
- [22] Huang Y and Yang V. Dynamics and stability of lean-premixed swirl-stabilized combustion. *Progress in Energy and Combustion Science* 2009; 35(4): 293–364.
- [23] O'Connor J, Acharya V and Lieuwen T. Transverse combustion instabilities: Acoustic, fluid mechanic, and flame processes. *Progress in Energy and Combustion Science* 2015; 49: 1–39.
- [24] Poinot T. Prediction and control of combustion instabilities in real engines. *Proceedings of the Combustion Institute* 2017; 36(1): 1–28.
- [25] Bourgooin JF, Durox D, Moeck JP et al. A new pattern of instability observed in an annular combustor: The slanted mode. *Proceedings of the Combustion Institute* 2015; 35(3): 3237–3244.
- [26] Bourgooin JF, Durox D, Moeck JP et al. Characterization and modelling of a spinning thermoacoustic instability in an annular combustor equipped with multiple matrix injectors. *Journal of Engineering for Gas Turbines and Power* 2015; 137: 021503.
- [27] Vignat G, Durox D, Renaud A et al. High amplitude combustion instabilities in an annular combustor inducing pressure field deformation and flame blow-off. *Journal of Engineering for Gas Turbines and Power* 2020; 142: 011016.
- [28] O'Connor J and Lieuwen T. Disturbance field characteristics of a transversely excited burner. *Combustion Science and Technology* 2011; 183(5): 427–443.
- [29] O'Connor J and Lieuwen T. Further characterization of the disturbance field in a transversely excited swirl-stabilized flame. *Journal of Engineering for Gas Turbines and Power* 2012; 134: 011501.
- [30] Kwong WY and Steinberg AM. Effect of internozzle spacing on lean blow-off of a linear multinozzle combustor. *Journal of Propulsion and Power* 2020; 36(4): 540–550.
- [31] Lespinasse F, Baillot F and Boushaki T. Responses of v-flames placed in an hf transverse acoustic field from a velocity to pressure antinode. *Comptes Rendus Mécanique* 2013; 341(1): 110–120.
- [32] Baillot F and Lespinasse F. Response of a laminar premixed v-flame to a high-frequency transverse acoustic field. *Combustion and Flame* 2014; 161(5): 1247–1267.
- [33] Hauser M, Lorenz M and Sattelmayer T. Influence of transversal acoustic excitation of the burner approach flow on the flame structure. *Journal of Engineering for Gas Turbines and Power* 2011; 133: 041501.
- [34] Baillot F, Patat C, Caceres M et al. Saturation phenomenon of swirling spray flames at pressure antinodes of a transverse acoustic field. *Proceedings of the Combustion Institute, Online* 2021; 38(5): 5987–5995.
- [35] Prieur K, Durox D, Beaunier J et al. Ignition dynamics in an annular combustor for liquid spray and premixed gaseous injection. *Proceedings of the Combustion Institute* 2017; 36(3): 3717–3724.